Journal of Hazardous Materials 440 (2022) 129779

Contents lists available at ScienceDirect

Journal of Hazardous Materials

journal homepage: www.elsevier.com/locate/jhazmat

Experimental evaluation of vertical metal retardation in stormwater management practices as influenced by cycles of baseline and high salinity

Ali Behbahani [a,b], Robert J. Ryan [a], Erica R. McKenzie [a,*]

[a] Temple University, Department of Civil and Environmental Engineering, 1947 North 12 Street, Philadelphia, PA 19122, United States
[b] F. X. Browne, Inc. / Bogia Engineering, Inc.1101 S Broad St, Lansdale, PA 19446

GRAPHICAL ABSTRACT

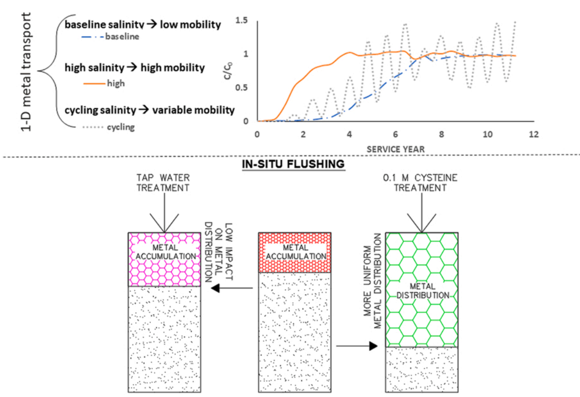

ARTICLE INFO

Editor: Y. Deng

Keywords:
Stormwater
NaCl effects
Metal mobility
Dynamic modeling
In-situ soil remediation

ABSTRACT

The application of NaCl as a deicer increases salinity of stormwater runoff, which may impact the speciation and mobility of various contaminants, including metals. Salt can remain in the fill media of stormwater management practices for an extended period after application, creating annual cycles of baseline and high salinity. This study evaluated the impacts of NaCl concentration and application cycles on metal retardation in fill media via 1-D continuous flow bench-scale columns. The high salinity scenario of 0.1 M NaCl decreased retardation factors of metals when compared to baseline salinity scenario of 0.01 M NaCl. Application of cycling baseline and high NaCl caused substantial fluctuations in the effluent metal concentration. The metals that were adsorbed during the baseline salinity periods were desorbed during the high salinity periods, leading to elevated concentrations of metals in porewater and effluent. Flushing with water removed only Na from the fill media top layers, while applying cysteine, as an environmentally friendly chelator, was demonstrated to be a promising approach to mobilizing accumulated metals from top layers to deeper layers. The results suggest that incorporating seasonal changes in environmental variables such as salinity enhances accuracy of contaminant transport modeling in fill media.

* Corresponding author.
E-mail address: ermckenzie@temple.edu (E.R. McKenzie).

https://doi.org/10.1016/j.jhazmat.2022.129779
Received 24 May 2022; Received in revised form 5 August 2022; Accepted 12 August 2022
Available online 17 August 2022
0304-3894/

1. Introduction

Stormwater runoff can be problematic due to the increased risk of flooding and the potential for contaminant washoff (Obropta and Kardos, 2007). Stormwater management is more challenging in urbanized areas because developed lands (i.e., impervious surfaces) can increase the likelihood of runoff and intensify its power to entrain built-up contaminants (Tang et al., 2021). Stormwater management practices (SMPs) are among low impact development approaches that have been widely employed to manage stormwater runoff to address quantity and quality concerns (Kratky et al., 2017). SMPs capture stormwater runoff from contributing drainage areas (e.g., roadways) and gradually drain it to either downstream infrastructure and water bodies (e.g., sewer system or surface streams) or groundwater, therefore, they have a potential of being a point source of contamination for water resources (Ivanovsky et al., 2018). A sustainable SMP design needs to holistically take into account the water quality enhancement before discharging the stormwater into water resources.

A variety of contaminants have been detected in stormwater runoff, including nutrients, metals, and sediments (Davis et al., 2001). Among these contaminants, sediments and metals can easily accumulate on impervious surfaces during dry periods (Wei et al., 2019). Metals are abundant and non-degradable constituents of urban runoff that have been regulated by many entities due to their potential toxicity (Anderson et al., 2016). Engineered soils selected for use in SMPs (e.g., loamy sand and sandy loam) often demonstrate good removal efficiencies for most of the environmentally important metals such as Cr, Cu, Ni, Cd, and Pb (Wang et al., 2016; Sangiumsak and Punrattanasin, 2014). However, metal retardation in the fill media can be impacted by various factors such as cation exchange capacity (CEC), pH, organic content, dissolved oxygen, and salinity (Augustine, 2017; Degryse et al., 2009). Acosta et al. (2011) demonstrated that runoff with higher salinity resulted in greater mobility of Cu, Zn, Cd, and Pb through the soil media. In addition to the chemistry of runoff and fill media, physical characteristics of fill media such as clay percentage may affect removal owing to high organic content and small size of clay particles which promote metal adsorption (Fonseca et al., 2011). It should be noted that in circumneutral environments such as stormwater runoff, the the exchangeable fraction of metals that is subject to retardation and/or mobilization (Tomczak et al., 2019; Boyer et al., 2018).

Stormwater management from both quantity and quality perspectives is typically addressed through static design approaches, which assume characteristics are constant over time. On the contrary, a dynamic approach takes into account temporal changes in characteristics. One parameter that governs metal removal during infiltration is the soil-water distribution coefficient (K_d), defined as the ratio of the solid-associated metal concentration to its aqueous phase concentration at equilibrium. Static metal transport models employ a fixed distribution coefficient, while real-world data suggest a fixed distribution coefficient may inaccurately estimate the capacity of fill media to retard metal transport. For instance, metal removal efficiency were notably reduced for Cu, Zn, and Cd in a SMP due to NaCl application in the wintertime (Kratky et al., 2017). The high Na concentration competes with cationic metals for sorption sites in the fill media, reducing metal distribution coefficients. Additionally, Cl will form complexes with previously adsorbed metals and release them, further reducing the distribution coefficient (Behbahani et al., 2021). A distribution coefficient that is responsive to environmental factors (i.e., dynamic) is a more realistic approach to understand and model metal fate and transport. It is particularly applicable in northern climates, where NaCl application in the wintertime and its extended presence in the fill media through spring, is unavoidable for safety reasons. However, the salt application is not limited to safety measures in northern climates and a high salinity condition can occur for an extended period in areas where salt is used as a dust suppressant (Parvej et al., 2021).

Several studies have investigated the impacts of salt on metal mobility through porous media (e.g., Paus et al., 2014), however, only a few of them have studied the cycling between high and baseline salinity periods (McManus and Davis, 2020). For instance, Paus et al. (2014) studied the impacts of high salt and low temperatures on the mobility of Cu, Zn, and Cd using experimental columns and found that applying 1000 mg/L NaCl solution increased the mobility of all studied metals through the porous media, while the low temperature decreased the mobility of Zn and Cd, and increased the mobility of Cu. McManus and Davis (2020) conducted column experiments to assess contaminant mobility in response to episodic high NaCl concentrations (2000, 5000, and 10,000 mg/L) as opposed to the baseline salinity of 20 mg/L. Each episode of high salinity was repeated after every six baseline salinity storms, and the elevated salinity resulted in higher porewater concentrations for all studied metals, nitrogen, and phosphorus. However, the highest metal concentrations in porewater were observed in the first and second baseline events after the high salinity event. They attributed these observations to salt presence not only during the high salinity application event but for an extended period of time afterward. Field studies have also found that elevated salt concentrations in SMP fill media persist beyond the freezing seasons (Flanagan et al., 2019; McKenzie et al., 2019). The current study attempted to experimentally monitor the impacts of cycles of baseline and high salinities, as opposed to constant or pulse-induced salinities, to mimic real-world situations more accurately.

The connection between elevated salinity and decreased sorption to the fill media presents a potential challenge for metal management in SMPs, however, it may also offer an opportunity for in-situ remediation techniques. Accumulation of metals in the top layers of the fill media has been observed in many SMPs (Walaszek et al., 2018; Anderson et al., 2016; Nieber et al., 2014). Although metal accumulation is an essential step for achieving water quality enhancement, it may also necessitate timely maintenance activities, especially if surficial media concentrations exceed regulatory values. Surficial soils with high concentrations of adsorbed metals pose the potential risk of metals becoming resuspended or redistributed. Fill media maintenance can include soil replacement, but this is relatively expensive and tedious, while in-situ remediation can be less expensive and faster. Generally, in-situ and ex-situ soil remediations (for metals) utilize chelators to release the metals from the soil particles (Bolan et al., 2014). While a concentrated NaCl solution may effectively mobilize metals, the resultant Cl contamination renders NaCl an inappropriate remediation approach. Dolev et al. (2020) studied the efficacy of environmentally friendly chelators like proteinogenic amino acids, including cysteine, for metal release in ex-situ experiments (i.e., batch experiments on disturbed soil). Cysteine released ~65 %, ~15 %, ~30 %, and ~40 % of the Cd, Cu, Ni, and Zn from the soil, respectively, which were notably higher than washing the soil with water (which recovered less than 5% for all studied metals). Decreasing the metal concentration in the top layers may reduce the risk of surficial resuspension and redistribution. Moreover, calcium (Ca) is an important element for plant health and was not released after applying cysteine (Dolev et al., 2020), while many other chelators such as EDTA can mobilize Ca (Zhang and Tsang, 2013). The current study included testing the potential of cysteine to flush down metals as an in-situ (i.e., undisturbed media) remediation technique. This type of approach (i.e., in-situ remediation) can be a promising and cost-effective tool to remediate the surface of SMP fill media, where high accumulation of contaminants occurs. These surficial contaminants are prone to resuspension and redistribution, posing the risk of contamination for surface water bodies. Applying a moderate and environmentally-, environmentally friendly chelator like cysteine may not only flush the surficial contaminants to the lower layers but also prevent them from being fully flushed from the fill media (i.e., minimize the risk of groundwater contamination).

Column experiments were conducted to investigate the impacts of baseline, high, and cycling salinities on the long-term retardation of a suite of metals (Cr, Mn, Fe, Cu, Zn, and Pb) for loamy sand media. These are metals that are abundant in the stormwater and of regulatory importance (standards that exist or are under review) in both aquatic and soil systems (US-EPA, 2002; US-EPA, 2003; US-EPA, 2017a; US-EPA, 2017b). Additionally, they can be categorized as potentially toxic elements (PTEs) due to their potential adverse impact on biota (Anderson et al., 2016). The effect of fill media characteristics was also considered, contrasting loamy sand and sandy loam in the cycling salinity scenario, to assess the potential difference in metal retardation. After reaching full breakthrough of metals in the top layers, flushing treatments of tap water and 0.25 M cysteine were applied to test the efficacy of each treatment to mobilize metals.

2. Materials and methods

2.1. Column construction and characteristics

Metal transport through the porous media was experimentally evaluated using 8 bench-scale columns that represented 4 different scenarios in duplicate, where the duplicates were designated as "A" and "B". Scenarios included: 1) static baseline salinity of 0.01 M (0.584 g/L) NaCl in synthetic stormwater (SSW) applied to loamy sand media, 2) static high salinity of 0.1 M (5.84 g/L) NaCl in SSW applied to the loamy sand media, 3) dynamic baseline and high salinity cycles of SSW applied to loamy sand media, and 4) dynamic baseline and high salinity cycles of SSW applied to sandy loam media. Each column was run for ~4 months to simulate ~14 years of real-world SMP service time. The cycling salinity condition was created by applying SSW with baseline salinity for 96 h and applying SSW with high salinity for another 96 h; each 96-h application window was equivalent to 6 months of SMP use (assuming a ratio of drainage area to the SMP infiltration area of 6 and Philadelphia annual precipitation records; more details in Supplementary data A). Characterization was performed to determine particle size distribution (PSD), exchangeable sodium percentage (ESP), cationic exchange capacity (CEC) and organic content. ESP is representative of sodic level, where ESP greater than 15 % is considered sodic fill media and not appropriate for SMP use. CEC is defined as total available negatively charged sites on the surface of particles that can bind with cations. Owing to substantial impact of CEC on metal sorption, there are some recommendations from agencies for the minimum required CEC of fill media in SMPs. For instance, Philadelphia stormwater management guidelines recommends employing fill media with at least 5 meq/100 g soil (City of Philadelphia Planning and Research and City of Philadelphia Water Department, 2014). The 1 M KCl extraction method was employed to estimate CEC of different samples (Ross and Ketterings, 2011). Organic content was estimated by the loss on ignition (LOI) method, and PSD was analyzed by using an LS 13 320 Particle Size Analyzer. Loamy sand media was composed of 85 % sand, 10 % silt, and 5 % clay; the organic content, ESP, and cationic exchange capacity were 2.5±0.21 %, 5.43±0.12 %, and 8.36±1.12 $\frac{meq}{100g}$, respectively. Sandy loam media was composed of 65% sand, 30% silt, and 5% clay; the organic content, ESP, and cationic exchange capacity were 3.7±0.54 %, 5.66±0.20 %, and 10.43±2.33 $\frac{meq}{100g}$, respectively. Table 1 summarizes the properties of SSW, which was prepared using deionized water (DI) with a resistance of 18.2 MΩ-cm and the averages of environmentally relevant concentrations that were observed during 4-years of stormwater monitoring in Philadelphia, PA, USA (McKenzie et al., 2019). The average and maximum Na concentration measured in stormwater runoff in the aforementioned SMP monitoring were converted to NaCl concentration and used in this study for baseline and high salinity, respectively. Additionally, the global average of event mean concentrations (EMC) of studied metals in the influent to SMPs were extracted from the International Stormwater BMP Database (2021) and are presented as a reference for comparison.

Columns were constructed using PVC pipes with an inner diameter (ID) of 10 cm and PVC endcaps. The total length of each column was 25 cm consisting of 15 cm of fill media (loamy sand or sandy loam) with 5 cm layers of gravel (grain sizes greater than 2.5 cm) on top and at the bottom (Fig. 1). Fill media and gravel layers were separated by a non-woven geotextile fabric (Underguard) to prevent the mobilization of fine particles during the experiment. The fill media was damp packed in 2.5 cm layers, where porous media consistency was promoted by scarifying the surface of the lower layer before adding the next one and placing an equal mass of fill media for each layer, which created consistent fill media porosity of ~ 0.45 in all columns. Micro lysimeters (SoilMoisture Equipment Corp.) with an outer diameter of 0.95 cm were installed into the packed fill media, per manufacturer instructions, to collect porewater samples at 5 and 10 cm below the surface of the fill media in an upward flow direction (Fig. 1), then the geotextile fabric and top gravel layer were installed, followed by the cap. Holes were drilled in the caps to pass through tubing (Cole Parmer, 3.2 mm ID silicone) and lysimeters. Adhesive sealant was used to create a watertight seal with

Table 1
Nominal concentrations, chemicals, and suppliers for synthetic stormwater; the Mean EMC column displays values reported from the international stormwater BMP database (2021).

	Value	Chemical	Supplier	Mean EMC
pH	7	HNO_3 & $KHCO_3$	Fisher Scientific & Aquaponic	7
TOC, mg-C/L	10	Humic acid	Sigma-Aldrich	19
Cr, μg/L	30	$Cr(NO_3)_3 0.9H_2O$	Sigma-Aldrich	8
Mn, μg/L	30	$Mn(NO_3)_2$	Sigma-Aldrich	117
Fe, μg/L	600	$Fe(NO_3)_3 0.9H_2O$	Sigma-Aldrich	1873
Cu, μg/L	60	$Cu(NO_3)_2 0.3H_2O$	Sigma-Aldrich	40
Zn, μg/L	150	$Zn(NO_3)_2 0.6H_2O$	Sigma-Aldrich	129
Pb, μg/L	7	$Pb(NO_3)_2$	Sigma-Aldrich	45
NaCl, g/L	0.58[a] & 5.8[b]	NaCl	Sigma-Aldrich	0.73[c]

[a] NaCl concentration in SSW with baseline salinity condition, equivalent to 0.01 mol/L.
[b] NaCl concentration in SSW with high salinity condition, equivalent to 0.1 mol/L.
[c] Mean EMC of total Na was converted to equivalent mean EMC of NaCl.

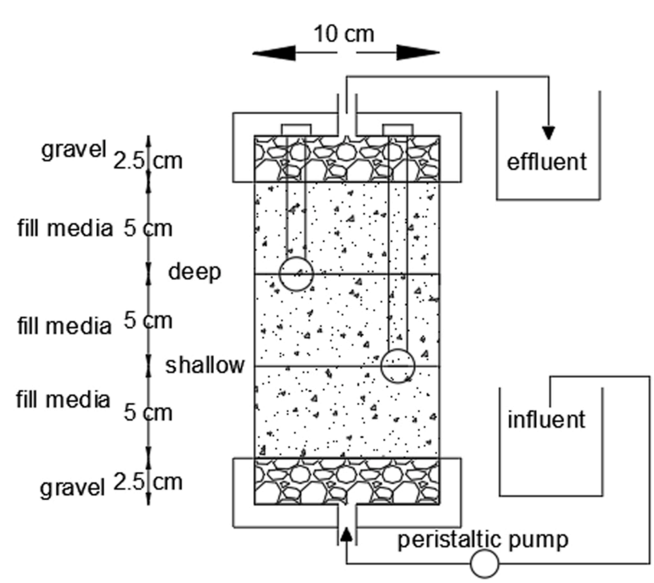

Fig. 1. Schematic of the column and water flow; shallow and deep lysimeters are defined based on the upward flow direction.

the endcaps and to prevent leakage from the holes.

2.2. Tracer test

Tracer tests were conducted for each column prior to and after the experiments to check the consistency of the water flow and fill media packing among the columns. A flow rate of 5 mL/min, which was equal to the main experiment flow rate, was used throughout the tracer test. Bromide (Br^-) was chosen as the tracer (250 mg/L Br solution, from KBr (Sigma-Aldrich), in DI water). Samples were collected from the effluent and analyzed using a Br^- selective electrode (Thermo Scientific). Retardation factor (R) of Br^-, median residence time, and dispersion coefficient were estimated from the tracer study by employing STANMOD (details in Section 2.5). An ideal tracer would have a retardation factor of 1 since theoretically, its distribution coefficient (K_d; $\frac{L}{kg}$) equals zero because it does not sorb to solids (Eq. 1). A threshold of ±10 % deviation in the estimated parameters (i.e., dispersion coefficient and retardation factor) was defined as the index of consistency among columns.

$$R = 1 + \frac{\rho K_d}{n} \tag{1}$$

In which, ρ $\left(\frac{kg}{L}\right)$ is the fill media dry bulk density and n the is fill media porosity.

Average R values, median residence time, and dispersion coefficient of all columns in the beginning and at the end of the experiment were 1.03 ± 0.01, 220.44 ± 7.44 min, and 0.012 ± 0.004 cm^2/min, respectively. The comprehensive report of tracer studies for each column is presented in Supplementary data B.

2.3. Influent application and sample collection

The long-term performance of the fill media was evaluated by applying a steady upward flow at 5 mL/min using a peristaltic pump at room temperature of ~20 °C. The upward flow was chosen to facilitate consistent saturated conditions and to limit potential hydraulic issues such as preferential flow paths and short-circuiting near the column inner walls (Paus et al., 2014). Equivalent service time was calculated from the experimental setup considering the following: fill media pore volume, applied accumulative influent volume, assumed loading ratio (6; ratio of contributing to infiltration area), assumed annual precipitation (Philadelphia region; 120 cm). An example calculation can be found in Supplementary data A, and for the stated assumptions, ~107 pore volumes corresponded to 1 year of service. The experiments were continued until full breakthrough for all the studied metals at the shallow lysimeters was reached.

The distance from the surface was defined using the geotextile fabric on the upgradient side as the datum (i.e., the surface of the fill media at the bottom of the column, closer to the influent; Fig. 1). Porewater samples were collected from shallow lysimeters (5 cm downgradient from the datum), deep lysimeters (10 cm downgradient from the datum), and effluent (15 cm from the datum) every 96 h, which was equivalent to the introduction of ~ 54 pore volumes of SSW (more details and an example calculation are in Supplementary data A). After each round of sampling, the salinity of cycling scenarios was altered, while salinities remained unchanged for baseline and high salinity scenarios throughout the entire experiment. All the scenarios were tested in duplicate columns, and randomly selected sample replicates were collected during each round of sampling. Vacuum syringes were used to extract samples from the lysimeters which were then transferred to 15 mL centrifuge tubes, while sampling from the effluent was collected directly into 15 mL centrifuge tubes. All the sampling components, including syringes and centrifuge tubes, were acid washed in a 5 % HNO_3 bath. After collection, samples were acidified with 0.5% HCl +2 % HNO_3 (v/v) and then stored at 4 °C until further analysis for metals.

2.4. Fill media flushing and post-experiment dissection

Series A columns were flushed with tap water, while series B columns were flushed with 0.25 M cysteine (assay > 99 % by Prescribed For Life) for ~ 27 pore volume over a period of 48 h after completion of the salinity experiments. The porewater and effluent samples were collected before and after the flushing procedure. The difference in the pre-and post-flush concentrations was used to evaluate the efficacy of each remediation solution (i.e., tap water and 0.25 M cysteine) to mobilize metals and Na.

After the flushing experiment, the columns were dissected, with fill media samples collected at 2.5 cm increments (i.e., 6 depths for each column). Fill media across the specified depth range was excavated using an acid-washed plastic scoop and was dispersed on a plastic sheet to air dry. After air-drying, the fill media was manually mixed and subsamples from the mixture were collected and stored at −20 °C until further processing. Samples were labeled based on the downgradient end of the layer (e.g., the subsample collection from the 2.5–5 cm segment was labeled as 5 cm below the surface). Next, the subsamples were oven-dried and the exchangeable metal concentrations were extracted using 1 M $MgCl_2$ in duplicate based on the method developed by Tessier et al. (1979). Exchangeable Na and metal concentrations (q (mg/kg); Eq. 2) were analyzed and data were used to evaluate remediation efficacy.

$$q = \frac{VC_w}{M} \tag{2}$$

in which, V (L) is the volume of extraction solution, C_w (μg/L) is the measured concentration in the extraction solution, and M (g) is the mass of fill media used in the extraction experiment.

2.5. Sample analysis and data processing

Elemental analysis was performed by an inductively coupled plasma mass spectrometry (ICP-MS; Agilent 7900). Although samples were analyzed for a suite of 54 elements, the targeted elements were Na, Cr, Mn, Fe, Cu, Zn, and Pb. Analytical interferences were minimized with helium and hydrogen gasses in the collision/reaction cells. Calibration curves were prepared from stock solutions (Inorganic Ventures), and values below the detection levels, which occurred mostly at the start of the experiment and in less than 5% of the samples, were assumed half detection level. Detection levels varied slightly based on the instrument tuning for each run, however, the average detection levels for Na, Cr, Mn, Fe, Cu, Zn, and Pb were 38.5, 0.5, 0.2, 0.7, 0.1, 0.2, and 0.03 μg/L, respectively. A threshold of ±30% deviation from target concentration for calibration points was considered acceptable. Sample analysis included three repeated measurements (MassHunter default settings) and the relative standard deviation (RSD) of concentrations derived from these measurements was checked to be less than 30%. A reference material (NIST 1640A) was run every 20 samples to check for accuracy and consistency. Moreover, the internal standard stability was monitored continuously (±30% acceptability threshold) with a maximum relative standard deviation of 5% for a sample's repeated measurements.

Porewater and effluent concentrations were inversely fitted with the analytical solution of the 1-D solute transport advection-dispersion-retardation equation (ADRE; Eq. 3) by employing STANMOD (van Genuchten et al., 2012). Eq. 3 assumes the system is advection dominated which was confirmed by Peclet numbers (Eq. 4) found to be orders of magnitude greater than 10 for metals (Appelo and Postma, 2005). The CXFIT model, which assumed zero production and degradation at an equilibrium state (i.e., reversible sorption processes occur instantaneously), was adopted to conduct the inverse fits. The data from each sampling depth were fitted separately and retardation factors (R values) for each metal and scenario were estimated. Retardation factors were estimated at all sampling locations where full breakthrough was observed.

$$\frac{C}{C_0} = 0.5\mathrm{erfc}\left(\frac{L\sqrt{R} - \frac{ut}{\sqrt{R}}}{2\sqrt{Dt}}\right) \tag{3}$$

$$Pe = \frac{uL^*}{D_f} \tag{4}$$

In which, C (μg/L) is the measured concentration at a specified sampling location, C_0 (μg/L) is the influent concentration, erfc is the complementary error function, L (cm) is the sampling depth, u (cm/min) is average linear velocity, t (min) is time, D (cm^2/min) is dispersion coefficient, Pe is Peclet number, L* (cm) is column characteristic dimension (defined as ratio of volume to area of column), and D_f (cm^2/min) is diffusion coefficient.

The dispersion coefficients were fitted based on the tracer test and then applied to the metal transport fitting. The coefficient of determination (r^2) for comparison between observed metal concentrations and theoretical metal concentrations from the analytical solution along with confidence bounds of R values were derived from STANMOD. A threshold of 0.95 for r^2 values was selected as an indicator of good fit.

The measured porewater metal concentrations in the cycling cases of loamy sand and sandy loam were compared using linear regressions. The regression parameters of r^2, slope, and intercept along with estimated confidence bounds were employed to assess the potential differences between the performance of each fill media type. The regression was performed on the data series from 5 cm below the surface during the entire course of the experiment. Confidence bounds of slopes were assessed and the difference between loamy sand and sandy loam was reported as significant when the confidence bound excluded 1.

Two-tail paired *t*-tests were conducted on the aqueous and solid-phase metal concentrations for statistical comparisons. The test was conducted on the solid-phase metal concentration (q) profile over depth to compare the tap water and cysteine treatments, and the paired parameter was q at each sampling depth. Moreover, the test was conducted to compare the time series of metal concentration (C) in porewater and at shallow depths derived from a transport model (Behbahani et al., 2020) with the experimentally measured concentrations; the paired parameter was C at shallow depth at each sampling time. The threshold for a significant difference was selected as a p-value smaller than 0.05 (i.e., 95% confidence level).

A mass balance was calculated for the metal introduced and retained in the column system. The total metal mass (M_{tot} (mg)), introduced to the system throughout the experiment, was calculated using Eq. 5, while the retained metal mass in the fill media after tap water and cysteine treatments ($M_{retained}$(mg)) was estimated using Eq. 6. The exported mass percentage (i.e., from the fill media) was calculated from M_{tot} and $M_{retained}$ using Eq. 7.

$$M_{tot} = 0.001C_0V_{tot} \tag{5}$$

$$M_{retained} = \sum_{i=1}^{6} M_i q_i \tag{6}$$

$$\text{exported mass}(\%) = \frac{M_{tot} - M_{retained}}{M_{tot}} \times 100 \tag{7}$$

In which, V_{tot} (L) is the total introduced SSW volume, i is the fill media layer number, M_i (kg) is the mass of the fill media in layer i, and q_i (mg/kg) is the exchangeable metal concentrations in layer i.

3. Results and discussion

3.1. Metal retardation in static baseline and high salinity scenarios

The high salinity scenario significantly decreased the retardation of all studied metals through the fill media compared to the baseline scenario. In the baseline salinity, Fe and Cu showed the highest retardations, reaching full breakthrough at shallow depths after 1520 pore volumes (Fig. 2a). Lead (Pb) was also notably retarded and reached full breakthrough at shallow depth after 1450 pore volumes in the case of baseline salinity. Full breakthrough of Cr at shallow depth was achieved after ~1000 pore volumes, indicating moderate retardation compared to Cu, Fe, and Pb. Such differences among retardation of studied metals were also observed in the high salinity scenarios, but the times to reach full breakthrough at 5 cm were substantially reduced to ~600 pore volumes, indicating lower retardation (Fig. 2b). Generally, Mn and Zn were abundant in the fill media and they leached substantially from the fill media, resulting in porewater and effluent concentrations exceeding the influent concentrations (i.e., $C/C_0 > 1$) in all tested scenarios (Fig. 2). Duplicate uncertainty, shown as standard deviations, are shown for different metals in various scenarios and depths in Supplementary data C (Fig. C4 to Fig. C27).

The porewater concentrations in the deep lysimeters and the column effluent also confirmed increased mobility of metals in high salinity conditions. For instance, Cr did not reach full breakthrough at either the deep lysimeters or the effluent in the baseline salinity, while full breakthrough of Cr at these sampling depths occurred after almost five years of service in the case of high salinity SSW (Fig. 3a). Similar trends were observed for Fe, Cu, and Pb, however, Fe reached only about 60% of its full breakthrough in the effluent under high salinity condition (Fig. 3b, c, d).

The rank order of R values associated with baseline salinity at shallow depth was (from greatest to least retardation) Cu > Fe > Pb > Cr, while this ranking changed to Fe > Cu > Pb > Cr in the high salinity scenario (Table 2). Such a shift between Fe and Cu in the ranking revealed the differences in the salinity effect on R values for these two metals. The R values of Cr, Fe, and Pb decreased by a factor of ~ 3 in the high salinity scenario, while the R value of Cu decreased by a factor of 4.3 (Table 2). Behbahani et al. (2021) conducted batch experiments to evaluate the impacts of salinity from different concentrations of various salts on metal K_d values. It was found that increasing the concentration of NaCl from 0.01 M to 0.1 M reduced the K_d values of Fe and Pb to a greater extent compared to Cr and Cu, while the current study suggested Cu was impacted more than other metals. Interactions between organic matter, which was included in the influent of the current flow-through study, and Cu may explain the reason; the SSW was not filtered or centrifuged before introducing it to the columns and therefore likely included particulate organic matter that could be retained on the top layer of the fill media. Organic matter impacts the mobility of Cu to a notable extent (Nelson et al., 2009; Blecken et al., 2009; Amrhein et al., 1992) and could immobilize Cu in the baseline salinity condition, resulting in higher retardation compared to other metals. However, particulate organic matter may also be subject to dissolution and higher mobility when exposed to a high salinity condition (Tedoldi et al., 2017; Wong et al., 2010). The greater influence of salinity on Cu vertical retardation may be derived from organic matter-induced transport.

Assessment of R values at multiple depths was feasible in the high salinity scenario because full breakthrough at deeper layers was achieved. Such assessment revealed that the retardation of metals at various depths was generally consistent, except for Cr which exhibited a significant decline in the R value from the shallow lysimeter to the effluent (Table 2). Generally, the goodness of fits and confidence bounds of R values were within the acceptable range of r^2 greater than 0.95 (Table 2), except for the cases of Mn and Zn for which substantial leaching from the media likely contributed to poorer fits. In both baseline and high salinity scenarios, the Zn concentration increased from shallow to effluent depths (Supplementary data C). Although Mn leaching was also observed throughout the media in both scenarios, the Mn concentrations decreased from shallow to effluent depths (Supplementary data C). The R values of Cr, Fe, Cu, and Pb were reliable owing to meeting the predefined statistical criteria (Section 2.5).

Potential changes in adsorption capacity of the fill media over depth

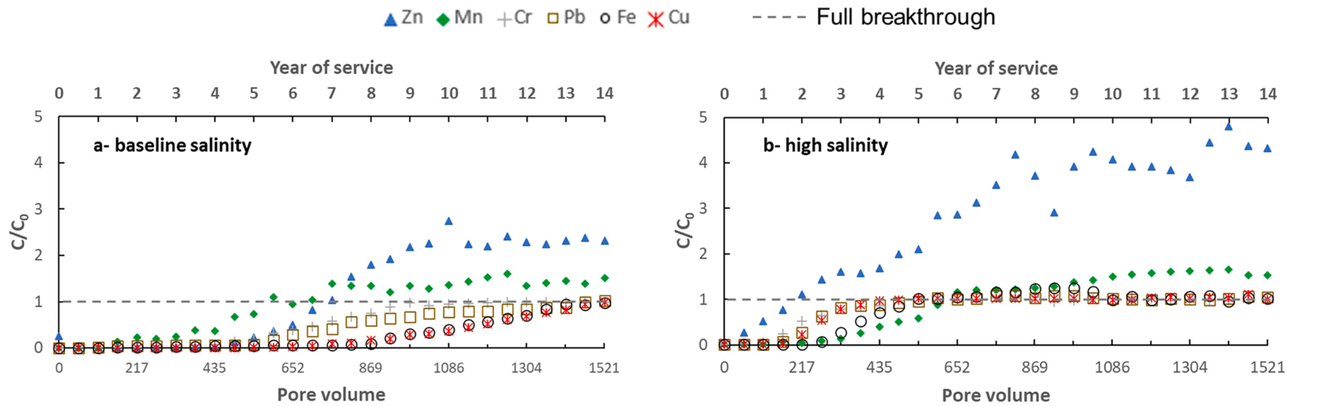

Fig. 2. Normalized porewater concentrations of studied metals at shallow depth (5 cm below the surface) for a- baseline salinity and b- high salinity; the averages of porewater concentrations from columns and their replicates were used.

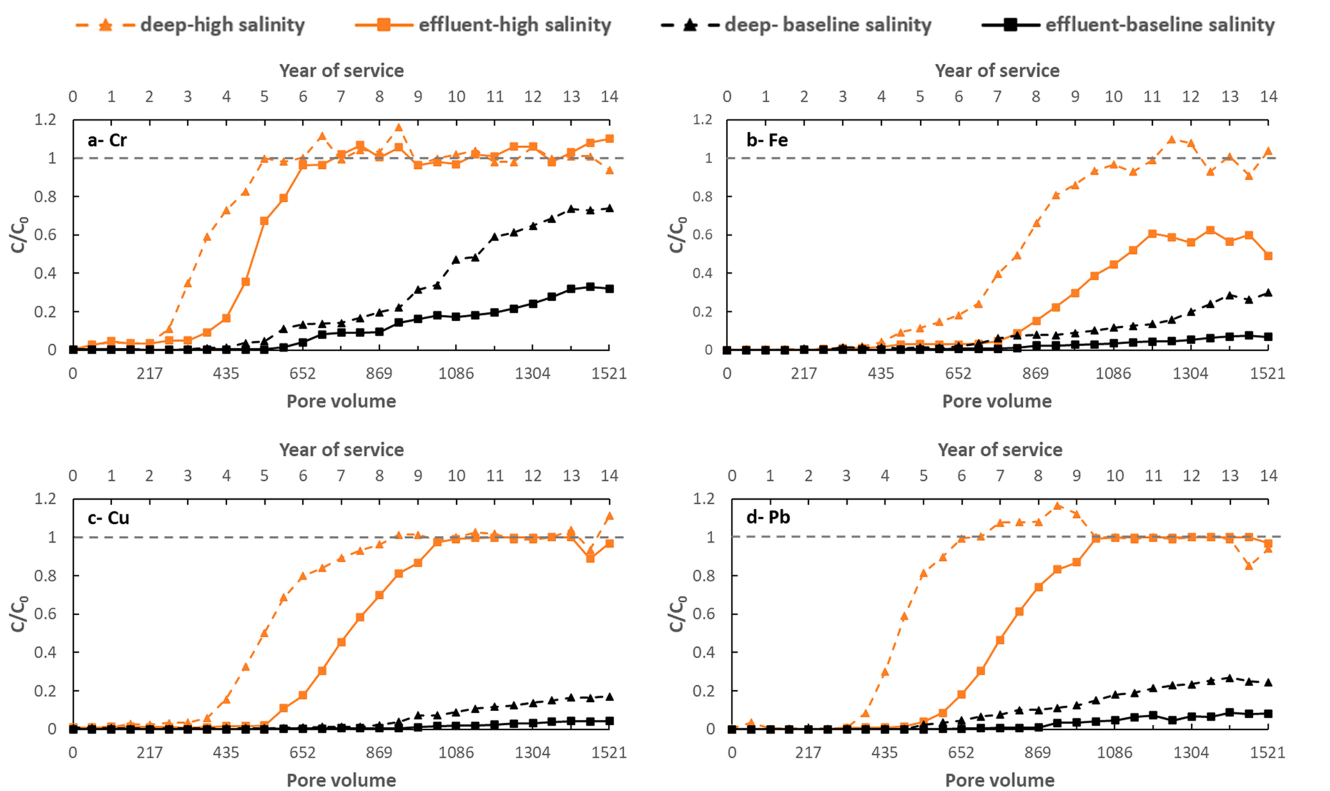

Fig. 3. Normalized porewater concentrations of metals at deep (10 cm below the surface) and effluent (15 cm below the surface) depths of baseline salinity and high salinity scenarios for a- Cr, b- Fe, c- Cu, and d- Pb; the averages of porewater concentrations from columns and their replicates were used.

may depend on a variety of factors, including depth-dependent trends in porewater concentrations of salt and metal, organic content, pH, oxidation-reduction potential, dissolved oxygen, and fill media particle size distribution (Tang et al., 2019; Wong et al., 2013; Acosta et al., 2011; Degryse et al., 2009; Norrström, 2005; Benoit and Rozan, 1999; Tessier et al., 1979). As water infiltrates, dissolved oxygen levels may decrease, resulting in more reducing conditions. Under reducing conditions, manganese hydroxide, which is an important soil functional group for metal adsorption (Kelly et al., 2020; Du Laing et al., 2009), may cause Mn (III) to be reduced to Mn (II), decreasing the capacity of the media for metal sorption. The release of Mn from the fill media even in the baseline salinity may suggest that such phenomenon occurred during the experiment because Mn (II) is more mobile than Mn (III) (Oldham et al., 2019; Luo et al., 2018). However, such changes in Mn speciation may have impacted Cr retardation to a greater extent compared to other cationic metals. As an oxyanion in a neutral environmental system (Benjamin, 2015), Cr interactions are different compared to other cationic metals. The adsorption of Cr is governed more by chemical bonds with soil functional groups than by electrostatic attraction onto the soil particles. Islam et al. (2020) reported soil functional groups bind with the inner and outer sphere chromate complexes, resulting in Cr adsorption, which might explain the significant decrease in Cr retardation over depth, while no significant trend for other metals was observed. However, additional studies are needed to more comprehensively test these potential mechanisms such as trends in dissolved/particulate organic matter, and media particle size distribution over depth. Longer columns would better facilitate this examination.

High salinity increased the mobility of metals because equilibrium sorption capacity was decreased in the presence of elevated salt

Table 2
Retardation factors (R values) of Cr, Fe, Cu, and Pb in shallow depth of baseline and various depths of high salinity along with their statistics, derived from CXFIT inverse fit. Values after" ± " represent the 95% confidence bound; NA stands for not applicable when a full breakthrough was not achieved.

	shallow- baseline salinity		shallow- high salinity		deep- high salinity		effluent- high salinity	
	R value	r^2	R value	r^2	R value	r^2	R value	r^2
Cr	1233 ± 26	0.99	396 ± 26	0.95	315 ± 12	0.97	293 ± 6	0.99
Fe	1957 ± 32	0.98	654 ± 46	0.95	688 ± 15	0.98	NA	NA
Cu	1995 ± 31	0.99	463 ± 12	0.99	469 ± 11	0.99	447 ± 8	0.99
Pb	1437 ± 59	0.95	444 ± 19	0.98	406 ± 12	0.98	443 ± 7	0.99

concentrations due to cation exchange and formation of chloro-metal complexes (Behbahani et al., 2021; Wong et al., 2013; Bradl, 2004). Behbahani et al. (2021) reported that under a scenario of 0.1 M NaCl concentration, cation exchange was the most important contributor to lower distribution coefficient values (K_d) of metals (i.e., less retardation). The dominant mechanism of metal adsorption to soil is the electrostatic attraction of cationic metals to the negatively charged surface of particles (e.g., loam and clay particles). The elevated concentration of Na competes with cationic metals at concentrations that are orders of magnitude lower, which reduces the metal adsorption onto soil particles (i.e., causing a reduction in K_d). Other studies have also reported increased metal mobility in response to salt application. Paus et al. (2014) investigated different fill media by treating columns with 1000 mg/L NaCl and found the effluent concentrations (15 cm below the surface) of Cd and Zn substantially increased after NaCl application, while Cu was less impacted by NaCl in media. As discussed previously, Cu was more impacted by salinity in the current study, potentially due to the presence of organic matter in the SSW used in the current study compared to organic matter-free influent for the column experiments by Paus et al. (2014). Søberg et al. (2017) tested the performances of different pilot-scale bioretention cells under baseline and high salinity conditions and found that metal mobility generally increased, resulting in lower removal efficiencies. They also observed cases of substantial leaching of Cu and Pb in the presence of high salt. Wen et al. (2019) studied the impacts of saline coastal water on groundwater quality and showed the higher salinity resulted in higher metal concentration and associated health risks, potentially due to elevated dissolved form of metals.

3.2. Metal retardation in dynamic cycling scenarios

Influent salinity cycling was associated with notable variations in the porewater concentrations in both loamy sand and sandy loam media, indicating fluctuations in the fill media sorption capacity and resultant metal retardation. As hypothesized and in line with the findings from Section 3.1, both media had substantially higher effluent and porewater metal concentrations, associated with lower metal retardation, during the high salinity periods for all the studied metals. Normalized porewater concentrations at shallow depth at the end of each cycle are shown in Fig. 4. The average porewater concentrations (average of baseline and high salinity scenarios) gradually increased and plateaued, similar to a classic breakthrough curve, suggesting that metals accumulated in the media over time. For samples associated with the high salinity periods, metal concentrations at shallow depths frequently exceeded the influent concentrations in the cycling scenarios, suggesting desorption from the media (Fig. 4). Zinc and Mn porewater concentrations were more notably affected by the dynamic cycling scenarios compared to static baseline and high salinities (Fig. C1 and C2 in Supplementary data C). Evidence of salinity-induced desorption was also exhibited by Cr, Fe, Cu, and Pb, which did not exceed $C/C_0 \sim 1$ during the static high salinity scenario. For instance, Pb porewater concentrations at the shallow depth in the dynamic cycling scenario of loamy sand media exceeded the influent concentration (i.e., $C/C_0 > 1$) after ~ 650 pore volumes (Fig. 4a), in corresponding pore volumes, Pb did not reach full breakthrough (i.e., $C/C_0 < 1$) in the static baseline salinity (Fig. 2a) and did not exceed the influent concentration in the static high salinity (Fig. 2b). This comparison is also depicted in Fig. C3 of Supplementary data C.

Higher metal adsorption during baseline periods resulted in elevated accumulation in the fill media. When the high salinity period began, these accumulated metals desorbed, leading to elevated porewater and effluent concentrations. High salinity periods not only undermined the ability of the fill media to adsorptively remove metals but also desorbed metals that had become solid-associate during the low salinity periods. This effect was not observed in the static high salinity scenario because the capacity of the fill media was consistently low, and a constant distribution coefficient governed the mass distribution between aqueous and solid phases. Metals such as Cr, Pb, Fe, and Cu, which did not have a substantial source in the fill media, only reached full breakthrough (i.e., equal incoming and outgoing concentration) in the static high salinity scenario. The changes in distribution coefficient, as a result of variations of salinity in dynamic cycling cases, resulted in the accumulation of metals in the fill media during baseline periods. Such accumulation acted as a source of metal during high salinity periods. The distribution of mass in the high salinity periods changed in favor of the aqueous phase, resulting in added metal mass to the incoming mass (i.e., desorption). This has important practical implications because roadway runoff may have highly variable salinities which are greatly influenced

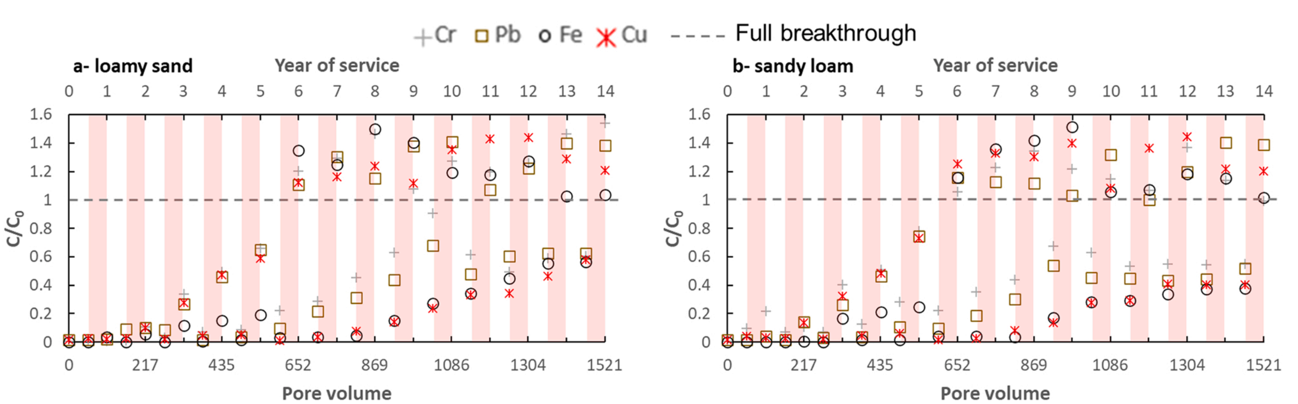

Fig. 4. Normalized porewater concentrations of studied metals at shallow depth (5 cm below the surface) of cycling scenario for a- loamy sand media and b- sandy loam media; shaded area represents the periods of high salinity application; the averages of porewater concentrations from duplicate columns are presented.

by salt employed as a deicer in northern climates or as a seasonal dust suppressant for unpaved roads. In either case, the stormwater runoff would flush the salt from the contributing surface to the SMP fill media, where the salt can remain for an extended period of time, creating a cycle of high salinity condition. Subsequent storms would eventually flush the salt from the SMP fill media, creating a baseline salinity cycle. This process cannot be modeled in a static approach that employs a constant retardation factor for the fill media. It highlights the importance of dynamic contaminant fate and transport modeling, which accounts for temporal variations due to environmental factors.

Applying dynamic R values to a previously developed contaminant transport model (Behbahani et al., 2020) revealed a similar fluctuating pattern when dynamic salinity was modeled. For instance, normalized Pb porewater concentration at 5 cm below the surface for two scenarios are shown in Fig. 5: a- dynamic cycling salinity scenario via applying rotating high and low R values (presented in dotted red line), and b- static salinity scenario via applying a constant R value that was the average of low and high R values of the high and baseline salinity scenarios (represented by black dashed line). In the static scenario, the fill media performance was overestimated in the high salinity condition or underestimated in the baseline salinity condition. Hence, even using an average R value could not predict the metal transport accurately. Although using a constant average R value may provide insight into gradual accumulation in the media, employing dynamic R values could more accurately model the real environmental systems. A paired two-tailed t-test was conducted to compare the measured porewater concentrations from the cycling experiments with those derived from the model. Generally, there was not a significant difference between the data sets, suggesting that the use of a different R value for low and high salinity components of the cycle reasonably reproduces the porewater concentrations. For instance, statistical comparison for Pb in the shallow depth between model and cycling salinity of loamy sand fill media yielded a p-value of 0.045 (Table D1 and Fig. D1 in Supplementay data D). The dynamics of the cycling salinities resulted in similar high fluctuation in concentrations at deep lysimeter and effluent sampling locations, similar to what was observed in the shallow lysimeters. The reduction in Fe concentrations at effluent relative to deep lysimeters was generally more notable than other metals (Fig. D3 in Supplementary data D), which might be due to differences in desorption mechanisms in presence of NaCl. Behbahani et al. (2021) showed that under 0.1 M NaCl treatment, formation of chloro-metal complexation did not effectively contribute to Fe desorption compared to cation exchange, while chloro-complexation played a more important role for desorption of Cr, Cu, and Pb. This suggests Fe is impacted by chloride-induced mobility to a lesser extent. Therefore, Fe desorption lacks one of the main mechanisms (i.e., complexation), resulting in limited desorption over depth when comparing to Cr, Cu, and Pb.

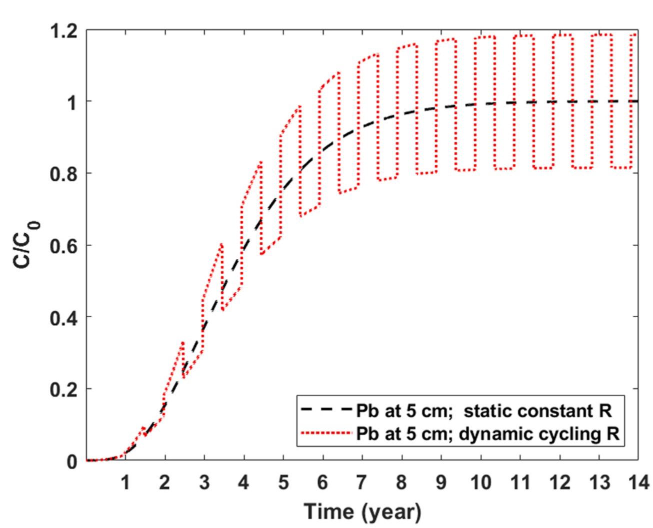

Fig. 5. Normalized porewater concentration of Pb at 5 cm below the surface, derived from a previously developed model (Behbahani et al., 2020) by using cycling and constant R values; the constant R value was the average of low and high R values that were used in the cycling scenario.

Limited differences were observed between the sandy loam and loamy sand porewater and effluent concentrations. Generally, the r^2 values, derived from the statistical regression analysis of porewater metal concentrations in loamy sand and sandy loam fill media under cycling salinity scenario, were greater than 0.95 for Cr, Fe, Cu, and Pb. The confidence bound of regression slopes included 1 for Mn, Fe, Cu, and Zn, suggesting an insignificant difference in porewater concentrations (Tables E1 - E4 in Supplementary data E). For instance, Fig. 6 and Table 3 presents the statistical analysis result for the case of Cr. As can be seen, porewater concentrations were slightly lower (<15 %) in the sandy loam media owing to greater adsorption, but the differences were significant for Cr (regression slope excluded 1). Lead (Pb) also revealed the same behavior as Cr (i.e., statistically significant difference when comparing loamy sand and sandy loam; Fig. E5 and Table E5 in Supplementary data E).

The statistical analysis to determine the significance of the difference was confirmed through another approach. The observed concentrations in sandy loam and loamy sand shown in Fig. 6 were rotated clockwise by 45° (i.e., transformed coordinates) to analyze the p-value of the regression slope. The transformed slope p-value represents the difference from a zero slope, which is equivalent to the difference from a slope of one (i.e., equal concentrations) in the real system shown above. For Cr, the slope regression p-value was 0.04, which indicates a significant difference between sandy loam and loamy sand. This p-value is in line with the 95 % confidence interval of the regression slope in Table 3 that excludes a slope of one.

The substantial fluctuations and episodic desorption observed for sandy loam and loamy sand suggest that there is not a practical difference in expected performance for metals removal in locations with seasonal salt application. Though the sandy loam media had 20 % more silt, higher organic content, and greater cationic exchange capacity, improved metal retardation was generally not observed. Therefore, practitioners may prefer loamy sand media (i.e., limit the amount of silt and clay to 15 %) to meet their infiltration rate and metal retardation interests. While increased fine particles in sandy loam did not notably improve metal retardation, elevated NaCl concentrations can induce stability of the fine particles (Behbahani et al., 2021) and clay dispersion (Oster et al., 2016), resulting in fill media clogging and decreased infiltration rates.

Haq et al. (2018) studied the impacts of episodic NaCl pulses on the

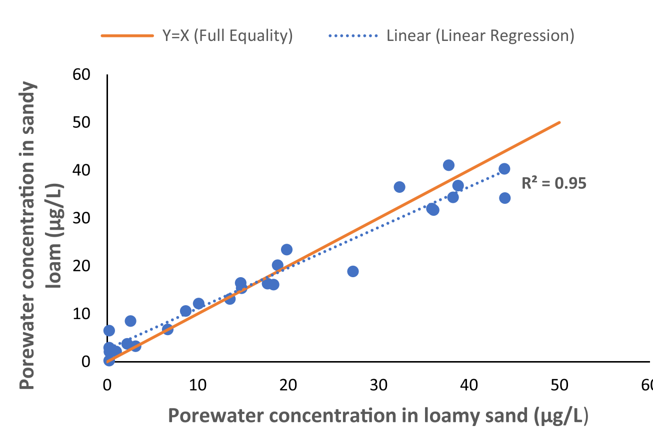

Fig. 6. Linear regression of measured Cr concentrations at the shallow sampling depth (i.e., 5 cm below the surface) of loamy sand and sandy loam media under cycling salinity scenario; samples were collected throughout the experiment.

Table 3
Statistical parameters derived from the regression between Cr concentrations at the shallow sampling depth (i.e., 5 cm below the surface) of loamy sand and sandy loam media under the cycling salinity scenario.

	Coefficients	Standard Error	Lower 95 %	Upper 95 %
Intercept	2.67	0.93	0.75	4.58
Slope	0.85	0.04	0.76	0.93

water quality of 12 large Eastern US watersheds and found significant trends of higher dissolved concentrations of cations, nutrients, phosphorus, and organic matter from hours to days after snowstorms that were followed by salt deicer application. Mullins et al. (2020) investigated seasonal patterns in the outflow of two infiltration-based green infrastructure (GI) sites in Pittsburg, PA, and recognized impacts of NaCl deicer as one of the main chemical drivers of the seasonal alterations in the GI performance, including substantially higher dissolved concentrations of metals such as Pb, Cu, Cd, and Zn as a response to NaCl application. McManus and Davis (2020) studied the impacts of periodic NaCl application (one high salinity event every 6 baseline salinity events) in experimental columns. They showed elevated concentrations of a range of contaminants, including metals, that occurred in the effluent during the first two events after the high salinity event (each event was equal to ~ 3 pore volumes, assuming a porosity of 0.45). This highlights that influent salt can change fate and transport of contaminants but also the retention of salt in the fill media is impactful.

Generally, mobility of metals can significantly increase in different environmental systems under high salinity conditions. For example, higher salinity enhanced the transport of metals in a river system (Zou et al., 2022). The impacts of salinity on metals adsorption/desorption behavior are not limited to the soil particles or stormwater management systems. For instance, Maity et al. (2021) studied the influential factors of metals adsorption onto micro and nano plastic particles and found high salinity decreased metal adsorption due to increased competition between electrolytes, resulting in increased ecotoxicity of the system. In similar research, Liu et al. (2022) showed the presence of either monovalent or divalent salts inhibited the adsorption of Pb (II) onto the surface of microplastics, though divalent salt limited the adsorption to a greater extent. A comprehensive statistical-based field and laboratory investigation of metal adsorption/desorption process in aquatic environments revealed that environmental factors such as pH and salinity affect the weakly-bound metals (i.e., exchangeable fractions); higher salinity and lower pH was associated with higher metal desorption, where pH was shown to be a more impactful statistical factor (Miranda et al., 2022).

3.3. Fill media flushing

Flushing with cysteine mobilized most metals compared to flushing with tap water. The analysis of fill media extracts for metals clearly showed lower concentrations in top layers (i.e., 2.5 cm below the surface; Figs. 7 and 8) for all the studied metals except Zn, after applying cysteine treatment when comparing to tap water treatment. Flushing with cysteine impacted the fill media exposed to baseline salinity to the greatest extent, while the lowest response was observed for the high salinity scenario. Since remediation is applicable and more relevant in case of high accumulation, the discussion in this section describes the fill media remediation experiments for the baseline salinity scenario, and the data for remediation experiments of other scenarios can be found in Supplementary data F. The fill media concentration profiles before flushing treatments were unavailable because the columns could not be dissected prior to flushing experiments. However, it is likely that the fill media concentration profile of tap water treatment in the baseline salinity scenario is reflective of the pre-treatment condition because the measured porewater concentrations before and after tap water treatments were essentially unchanged (Fig. G1 and G2 in Supplementary data G; all scenarios presented in Supplementary data G). For reference, the metal concentration profiles from the tap water-flushed system are shown in Fig. 7a (x-axis is a log scale), which shows that metals concentrations decreased with depth.

When the cysteine treatment was applied, two important alterations occurred in the metal concentration profiles. Firstly, the metal concentration profiles changed in response to the cysteine treatment, resulting in a quasi-increasing depth profiles (Fig. 7b; x-axis is a log scale) due to metal mobilization. A linear regression model was employed to quantify

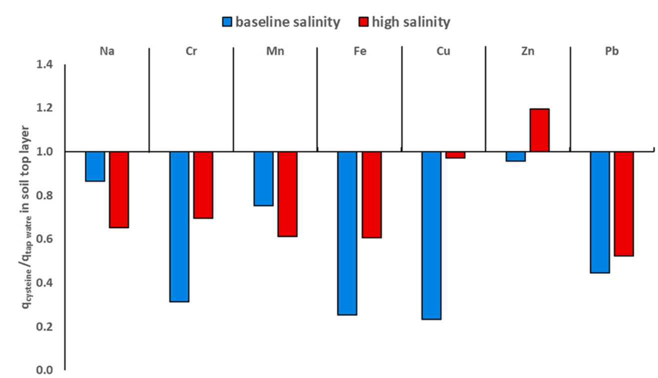

Fig. 8. The ratio of exchangeable concentrations in the fill media (q) after flushing with cysteine to corresponding values after flushing with tap water at the top layer of columns (i.e., 2.5 cm below the surface).

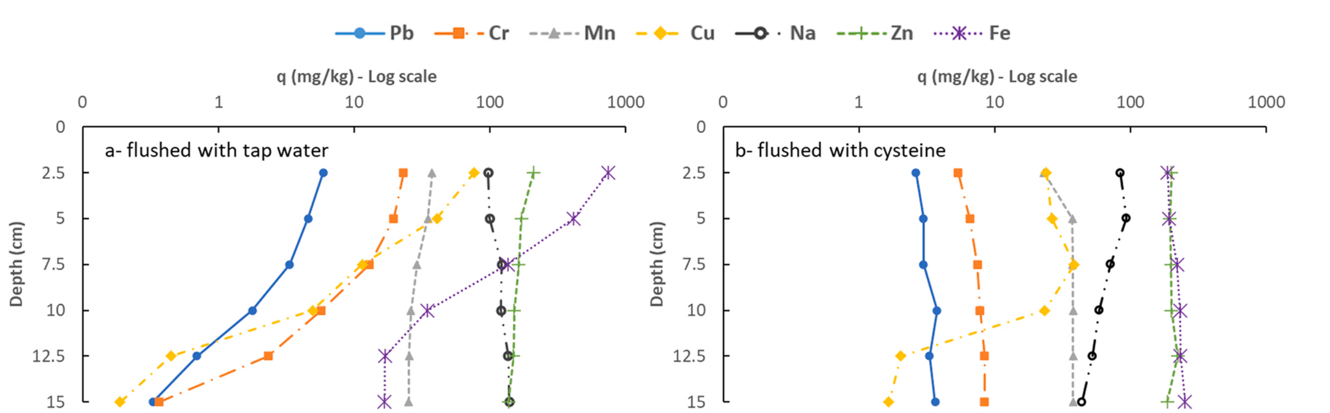

Fig. 7. Concentration (q) profile of Na and studied metals over depth of the fill media for a) tap water treatment and b) cysteine treatment for the baseline salinity scenario; each point is the average of duplicate sampling; the x-axis is in Log scale.

the changes in the metal concentration profiles in the fill media after flushing with tap water and cysteine. In this regression model (Eq. 8), the metal concentration in the fill media (q, mg/kg) was the dependent variable, and depth (d, cm) was the independent variable.

$$q=ad+b \quad (8)$$

In which a (mg/(kg.cm)) is the regression slope and b is the regression intercept.

A negative slope refers to decreasing concentration over the fill media depth, while a positive slope refers to an increasing trend. The impacts of tap water or cysteine treatments were evaluated by comparing the slopes associated with each treatment. The significant difference was defined as cases in which the confidence bound of estimated slopes did not overlap. The qualitative assessment of the concentration profiles, which indicated the concentration profiles changed from decreasing to quasi-increasing after treating with cysteine, was confirmed by the quantitative evaluation in almost all cases (i.e., more positive slope; except Cu in high salinity scenario; Fig. 9c). However, increased slope values were significant only in the baseline salinity scenario for all metals, and there were cases such as Fe and Cu in high salinity and Cu and Pb in cycling salinity of sandy loam that did not show a significant increase in the regression slopes (Fig. 9). Cr is an example to the contrary, where the slope in the baseline salinity scenario significantly increased from $-1.96 \frac{\text{mg}}{\text{kg.cm}}$ in the tap water treatment case to $0.24 \frac{\text{mg}}{\text{kg.cm}}$ in cysteine treatment (Fig. 9). A negative slope showed decreasing concentration trend in the concentration profile, while a positive slope indicated an increasing trend in concentration over depth.

Secondly, the metal concentrations in the fill media top layer (i.e., 2.5 cm below surface) of cysteine treatment notably dropped compared to their corresponding values from tap water treatment (Figs. 7 and 8). After flushing the baseline salinity column with 0.25 M cysteine solution for ~ 27 pore volumes, concentrations of exchangeable Cr, Fe, Cu, and Pb in the top layers of fill media decreased by factors of 3.3, 4, 5, and 2.5, respectively. For instance, Pb concentration notably decreased from ~ 5 mg/kg at 2.5 cm below the surface in the tap water treatment (Fig. 7a) to ~2 mg/kg in the cysteine treatment (Fig. 7b), suggesting that cysteine mobilized Pb from the top layer more than tap water. Additionally, statistical analysis (two-tail paired t-test on concentration profiles shown in Fig. 7) revealed that cysteine was significantly (i.e., p-value $<$ 0.05) more efficient in flushing Cr, Fe, Cu, and Pb in the baseline scenario (Table 4).

The concentration of Na in the top layer of baseline and high salinity scenarios decreased from ~100 mg/kg in the tap water treatment to ~72 mg/kg in the cysteine treatment, respectively (Fig. 7). However, the paired t-test analysis of the concentration profiles did not show a significant difference of treatments on the Na concentration profile in baseline salinity condition ($p > 0.05$; Table 4). Such insignificant impact from cysteine suggested applying tap water can effectively flush Na from the top layers and there is no need to apply a chelator for this purpose.

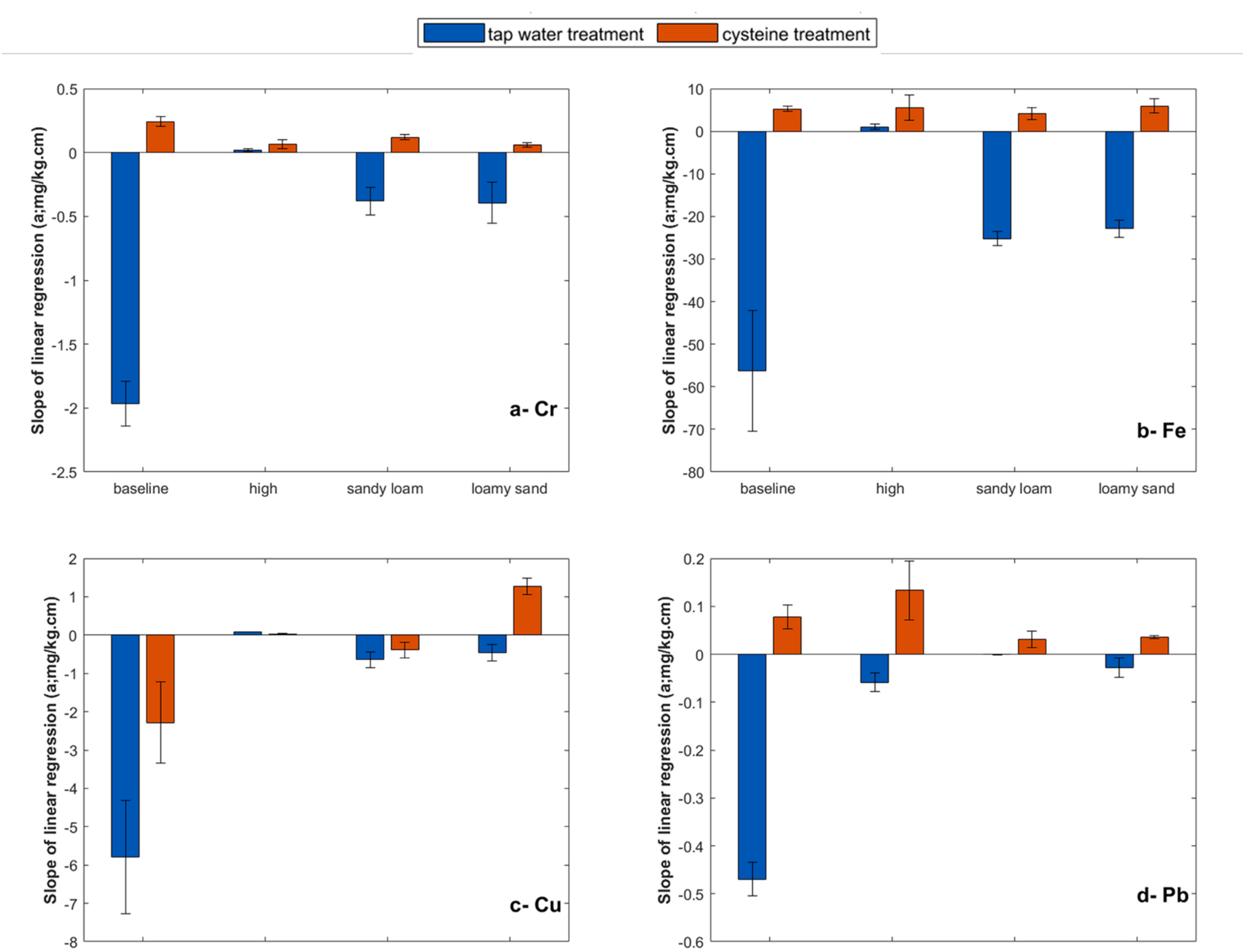

Fig. 9. The slope of the regression model after treating with tap water and cysteine under baseline salinity, high salinity, cycling salinity in loamy sand, and cycling salinity in sandy loam for a- Cr, b- Fe, c- Cu, and d- Pb; error bars represent standard error.

Table 4
p-values derived from the paired t-test of concentration profiles over depth after flushing with tap water and cysteine for all the studied scenarios.

	baseline salinity	high salinity	cycling - loamy sand	cycling - sandy loam
Na	0.13	<0.01	<0.01	<0.01
Cr	<0.01	0.16	0.02	0.69
Mn	0.32	0.68	0.03	0.46
Fe	0.03	0.42	0.70	0.56
Cu	<0.01	0.02	0.26	0.53
Zn	0.87	0.16	0.03	<0.01
Pb	<0.01	0.12	0.34	0.21

Impacts of cysteine in remediation of the top layer as a ratio between the two treatments based on the solid-associated concentrations in the top layer of the fill media is summarized in Fig. 8. Sodium (Na) and all the studied metals were moderately mobilized by cysteine from top layers, indicated by ratios smaller than 1. It can be concluded that employing cysteine can remediate top layers of the fill media and it can be significantly more effective during baseline salinity seasons (i.e., summer and fall), most likely due to higher metal accumulation.

The study of the metal mass balance over the 15 cm depth of the installed fill media indicated that metal mobilization due to cysteine treatment did not result in substantial export of metals from the effluent in the baseline salinity scenario. Total incoming and fill media retained masses for Cr, Fe, Cu, and Pb after tap water and cysteine treatments are shown in Fig. 10 for the baseline and high salinity scenarios. These metals were effectively retained in the baseline salinity and were present at low concentrations in the effluent samples, which suggested the majority of the total introduced metal loads were sorbed onto the fill media during the baseline condition. This is consistent with low effluent concentrations observed throughout the experiments shown in Fig. 3. The minimal difference between total introduced mass and retained mass after tap water treatment in the baseline scenario also confirms that the fill media concentration profile of the baseline salinity scenario after tap water treatment is a good approximation of the pre-treatment condition. Interestingly, the retained mass of metals after cysteine treatment was not substantially different from those treated with tap water (Fig. 10), suggesting that the metals were relocated within the column fill media but not substantially exported. Cysteine treatment resulted in exporting 29 %, 3 %, and 13 % of the available mass of Cr, Fe, and Cu, respectively (Table F1 in Supplementary data F). The mass of Pb in the fill media increased slightly (i.e., 16 %) after cysteine flushing, which might be due to uncertainties associated with the mass balance approximations such as heterogeneity of the fill media subsampling.

The chelation provided by 0.25 M cysteine treatment showed moderate evidence of remediation of the top layers. Stronger chelators were not tested in these experiments but they may mobilize the previously captured metals in an uncontrolled manner, including exporting them out of the fill media layer. Employing a strong chelator may require a porewater collection system in SMPs to collect exfiltrating contaminated porewater before reaching underlying groundwater. Optimal (i.e., optimal concentration and volume of treatment solution) application of a moderate chelator such as cysteine may mobilize the metals from the surface to deeper layers of the fill media in a controlled condition. Exported metal mass in high salinity and cycling scenarios were higher than baseline due to reduced retardations (Fig. 10, Fig. F3, and Fig. F5 in Supplementary data F). However, the comparison between tap water and cysteine treatments revealed notable differences in exports after cysteine treatment in cycling sandy loam versus those of baseline, high, and cycling cases for loamy sand (Table F1 in Supplementary data F). Cycling salinity scenario applied to sandy loam media was the only case that showed notable export of mass (i.e., from 25 % to 53 %) after treating with cysteine, which might be attributed to added 20 % loam in this type of fill media (Table F1 and Fig. F5 in Supplementary data F). This finding suggests caution should be taken for cysteine treatment when the fill media is comprised of more than 15 % loam.

The amine (-NH_2), thiol (-SH), and hydroxyl (-OH) functional groups in the cysteine structure are the chelating agents that can bind with metals in the fill media, resulting in a phase transfer from solid-associated to the aqueous. It should be noted that cysteine is not known to be a toxic compounds for environmental systems when present in concentrations of 0.25 M. Stability constants of metal-cysteine complexes (i.e., Log β, defined as the logarithm of the equilibrium constant for the complexation reaction between cysteine and metal; Benjamin, 2015; Berthon, 2007) are greater than those of metal-tap water because tap water does not contain amine and thiol. The cysteine solution was made from mixing cysteine in tap water. Therefore, cysteine solution contained extra chelating agents beyond those present in tap water, facilitating greater formation of metal complexes. Metal oxidation state impacts its complexation with ligands, including cysteine. Chromium, Mn, and Fe are mostly present in the soil in an oxidation state of III, while Cu, Zn, and Pb can be found in soil in an oxidation state of II (Kelly et al., 2020; Wuana and Okieimen, 2011). Considering these oxidation states, the metal-cysteine stability constants in the form of Log β can be ranked as Cr > Zn > Pb > Cu > Fe > Mn (Berthon, 2007). The mobilization of metals in the current study, represented by changes in porewater concentrations in the shallow depths, reported in Fig. G1 in Supplementary data G, did not fully follow the rank of stability constants (which was observed to be Cu > Fe > Cr > Pb > Mn > Zn in the baseline salinity of the current study; Figs. 7 and 8). This may partially be attributed to sampling over the depth of the columns and exposure to NaCl as opposed to batch tests that had been conducted to estimate stability constants in the study by Berthon (2007). The presence of fill media and NaCl potentially changes the chemistry compared to batch experiments, which did not include those, to estimate the stability constants. Nevertheless, more robust column studies coupled with batch experiments and speciation modeling need to be implemented to better

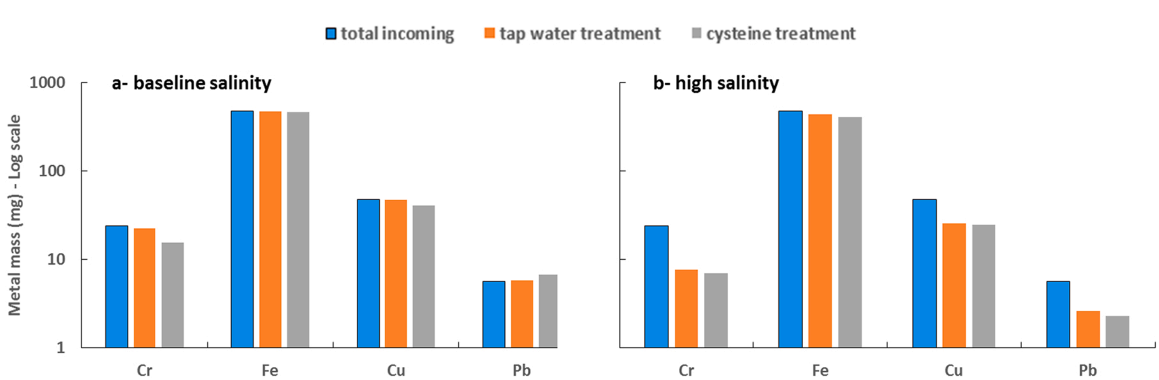

Fig. 10. Mass of Cr, Fe, Cu, and Pb associated with the total introduced SSW, and retained in the entire fill media (i.e., 15 cm fill media) after tap water and cysteine treatment for the a- baseline salinity and b- high salinity scenarios; y-axis is in the Log scale.

understand the mechanisms and implications of cysteine application for metal mobilization in stormwater management fill media.

Dolev et al. (2020) investigated the efficacy of a group of proteinogenic amino acids, including cysteine, in ex-situ soil remediation, and showed the moderate potential of cysteine to remediate contaminated soil from Cd, Ni, Zn, and to a lesser extent from Cu. They also demonstrated that proteinogenic amino acids can be considered environmentally friendly chelators because unlike stronger metal extractors (e.g., EDTA and HCl), they did not extract Ca and did not change the particle size distribution of soil. Liu et al. (2018) did a comprehensive review of different in-situ and ex-situ soil remediation methods and reported in-situ soil flushing can be a non-invasive, low-cost soil remediation technique but may have a potential risk of groundwater pollution. The results from the current study revealed that employing cysteine, a moderate chelator, as an extraction treatment for in-situ soil remediation, may mobilize metals only to a limited extent to clean the top layer as well as create a more evenly distributed concentration profile over the fill media depth. A cleaner fill media top layer may substantially lower the risk of surficial contamination resuspension, which is a probable scenario in SMPs under certain conditions such as high intensity storms (Behbahani et al., 2022). However, more investigation is still needed to optimize the concentration and volume of extraction treatments based on the site specification (e.g., fill media depth and degree of metal contamination), as well as to test the functionality of other amino acids for in-situ soil remediation. Additionally, maintaining plant health by cleaning part of the root zone, which depends on the plant type, may be achieved by determining the optimal treatment that allows metal mobilization to desired depths.

3.4. Environmental implications

Application of NaCl as a safety measure in northern climates as well as a seasonal dust suppressant results in higher salinity stormwater runoff, challenging the capability of SMPs to improve water quality through sorbing metal. This study showed the importance of improving the contaminant transport models to dynamically simulate the environmental factors (e.g., salinity). The results of the tested media in this research demonstrated adding loam (clay+silt) to the composition of engineered fill media in amounts higher than 15 % does not practically increase metal retardation when long-term salinity cycling is expected. Fine sediments are susceptible to clay dispersion when exposed to high concentrations of NaCl and this can adversely impact the infiltration capability of the fill media. Therefore, limiting the amount of loam in engineered fill media in northern climates can be an option to maintain infiltration rate while meeting metal retardation goal. Low-cost in-situ fill media remediation can be performed by applying cysteine as an environmentally friendly metal chelator in late summer/fall (under baseline salinity condition). Also, flushing the SMP fill media with water in early spring (after freezing season) can moderately clean the top layers of the fill media from salt. Flushing down metals and salt from top layers is an easy and helpful maintenance activity that can impede surficial resuspension and redistribution of contaminants.

The dynamic transport modeling can be extended by considering other environmental factors (e.g., organic content, DO, pH, etc.) beyond salinity. It should be noted that testing salinity was less complicated due to the seasonal patterns, while variability in the other water quality parameters may be more random. A suggested next step to improve the accuracy of the transport model is incorporating the role of various cysteine concentrations in the mobility of metals. Similar to what was performed for salinity, potential impacts of organic matter on the metal distribution coefficient can be studied by batch and column experiments, and the outcome may be applied in the transport models to predict the mobilities under various scenarios. Also, optimization of treatment approach (type and concentration of chelator, as well as application amount) can be achieved through batch and column experiments to evaluate various in-situ treatment goals.

4. Conclusion

Column experiments were implemented to evaluate the impacts of baseline, high, and cycling NaCl salinity on metal retardation through the SMP fill media. The baseline salinity scenario provided the highest retardation for metals, while retardation factors were notably reduced in the high salinity scenario due to competition for sorption sites between metals and Na that was present at concentrations several orders of magnitude higher. Since Na can remain in the fill media for an extended period of time, the high salinity scenario followed by baseline salinity was tested in a cycling manner to mimic a real-world situation. Cycling periods of high and baseline salinity may result in high fluctuation of metal porewater concentration in the fill media; low concentrations (i.e., comparatively efficient metal retardation) during baseline salinity, and high concentrations (i.e., comparatively inefficient metal retardation) during high salinity. The metals captured during the baseline salinity were released during high salinity, causing effluent concentration to exceed the influent concentration (i.e., due to reduced retardation), resulting in deteriorated water quality.

The cycling salinity scenario was applied to loamy sand (15 % silt+clay) and sandy loam media (35 % silt +clay). Statistical analysis showed significantly better retardation of Cr and Pb in the sandy loam media and no significant difference in Mn, Fe, Cu, and Zn retardation. Regardless of statistical significance, sandy loam media only showed slightly (<15 %) higher metal retardation. However, the higher retardation of metals was practically unimportant because the elevated salinity condition desorbed the accumulated metals.

Cysteine, a proteinogenic amino acid, was tested as an in-situ soil remediation technique. It was found that 0.25 M cysteine solution could moderately mobilize metals from the top layers of the fill media and transport them to the deeper layers. Fill media remediation was more efficient under the baseline salinity scenario and for metals with low background concentrations in the fill media due to the reduced concentration of these metals in the top layer of the fill media. Flushing the columns with tap water was not effective in mobilizing the metals but it was practically effective in mobilizing Na from the top layers.

CRediT authorship contribution statement

Ali Behbahani: Conceptualization, Methodology, Validation, Formal analysis, Investigation, Data Curation, Writing – original draft, Visualization. Robert Ryan: Validation, Data curation, Writing – review & editing, Supervision, Funding acquisition. Erica McKenzie: Conceptualization, Resources, Data curation, Writing – review & editing, Supervision, Project administration, Funding acquisition.

Declaration of Competing Interest

The authors declare that they have no known competing financial interests or personal relationships that could have appeared to influence the work reported in this paper.

Data availability

Data will be made available on request.

Acknowledgments

This research was funded by the Pennsylvania Department of Transportation (contract number 44000111660). We also would like to thank Janki Shah, the quality control manager at ALLAN MYERS, for providing us with the topsoil from a quarry located in Paradise, PA, USA. Recommendations and opinions included in this work are of the authors and do not necessarily reflect the opinions of PennDOT.

Environmental implication

Potentially toxic elements (e.g., metals) in stormwater pose a contamination risk to receiving water bodies, therefore, they are regulated by various agencies. While stormwater management practices (SMPs) are designed to address stormwater quantity and quality challenges, but contaminant removal is often assumed to be consistent. This research demonstrates that changes in salinity substantially changes metal retardation; seasonally elevated salinity can release metals captured during low salinity periods. Dynamic incorporation of environmental variations into the design of SMP fill media improves the accuracy of models to predict metal fate and transport, resulting in their higher functionality in water quality enhancement.

Appendix A. Supporting information

Supplementary data associated with this article can be found in the online version at doi:10.1016/j.jhazmat.2022.129779.

References

Acosta, J.A., Jansen, B., Kalbitz, K., Faz, A., Martínez-Martínez, S., 2011. Salinity increases mobility of heavy metals in soils. Chemosphere 85, 1318–1324. https://doi.org/10.1016/j.chemosphere.2011.07.046.

Amrhein, C., Strong, J.E., Mosher, P.A., 1992. Effect of deicing salts on metal and organic matter mobilization in roadside soils. Environ. Sci. Technol. 26, 703–709. https://doi.org/10.1021/es00028a006.

Anderson, B.S., Phillips, B.M., Voorhees, J.P., Siegler, K., Tjeerdema, R., 2016. Bioswales reduce contaminants associated with toxicity in urban storm water. Environ. Toxicol. Chem. 35, 3124–3134. https://doi.org/10.1002/etc.3472.

Appelo, T., Postma, D., 2005. geochemistry, Groundwater and Pollution, 2nd ed. CRC Press, Leiden, Netherland.

Augustine, A., 2017. Adsorption-desorption Study of Heavy Metals on Sandy-loam Soil of Sapele Metropolis 11, 17–27. https://doi.org/10.9790/2402-1108011727.

Behbahani, A., Ryan, R.J., McKenzie, E.R., 2020. Long-term simulation of potentially toxic elements (PTEs) accumulation and breakthrough in infiltration-based stormwater management practices (SMPs). J. Contam. Hydrol. 234, 103685 https://doi.org/10.1016/j.jconhyd.2020.103685.

Behbahani, A., Ryan, R.J., Mckenzie, E.R., 2021. Impacts of salinity on the dynamics of fine particles and their associated metals during stormwater management. Sci. Total Environ. 777, 146135 https://doi.org/10.1016/j.scitotenv.2021.146135.

Behbahani, A., McKenzie, E.R., Ryan, R.J., 2022. Impacts of size distribution and storm intensity on the behavior of suspended particles and their associated metals in a bioswale stormwater control measure. J. Sustain. Water Built Environ. 8 (3) https://doi.org/10.1061/jswbay.0000984.

Benjamin, M.M., 2015. Water Chemistry, Second ed.,. Waveland Press, Inc, Long Grove, IL, USA.

Benoit, G., Rozan, T.F., 1999. The influence of size distribution on the particle concentration effect and trace metal partitioning in rivers. GCA 63 (1), 113–127. https://doi.org/10.1016/S0016-7037(98)00276-2.

Berthon, G., 2007. Critical evaluation of the stability constants of metal complexes of amino acids with polar side chains (Technical Report). Pure Appl. Chem. 67, 1117–1240. https://doi.org/10.1351/pac199567071117.

Blecken, G.T., Zinger, Y., Deletić, A., Fletcher, T.D., Viklander, M., 2009. Impact of a submerged zone and a carbon source on heavy metal removal in stormwater biofilters. Ecol. Eng. 35, 769–778. https://doi.org/10.1016/j.ecoleng.2008.12.009.

Bolan, N., Kunhikrishnan, A., Thangarajan, R., Kumpiene, J., Park, J., Makino, T., Kirkham, M.B., Scheckel, K., 2014. Remediation of heavy metal(loid)s contaminated soils - To mobilize or to immobilize? J. Hazard. Mater. 266, 141–166. https://doi.org/10.1016/j.jhazmat.2013.12.018.

Boyer, P., Wells, C., Howard, B., 2018. Extended Kd distributions for freshwater environment. J. Environ. Radio. 192, 128–142. https://doi.org/10.1016/j.jenvrad.2018.06.006.

Bradl, H.B., 2004. Adsorption of heavy metal ions on soils and soils constituents. J. Colloid Interface Sci. 277, 1–18. https://doi.org/10.1016/j.jcis.2004.04.005.

City of Philadelphia Planning and Research, and City of Philadelphia Water Department. 2014. "Stormwater Management Guidance Manual." (July): 5–6.

Davis, A.P., Shokouhian, M., Sharma, H., Minami, C., 2001. Laboratory study of biological retention for urban stormwater management. Water Environ. Res. 73, 5–14. https://doi.org/10.2175/106143001×138624.

Degryse, F., Smolders, E., Parker, D.R., 2009. Partitioning of metals (Cd, Co, Cu, Ni, Pb, Zn) in soils: concepts, methodologies, prediction and applications - a review. Eur. J. Soil Sci. 60, 590–612. https://doi.org/10.1111/j.1365-2389.2009.01142.x.

Dolev, N., Katz, Z., Ludmer, Z., Ullmann, A., Brauner, N., Goikhman, R., 2020. Natural amino acids as potential chelators for soil remediation. Environ. Res. 183, 109140 https://doi.org/10.1016/j.envres.2020.109140.

Du Laing, G., Rinklebe, J., Vandecasteele, B., Meers, E., Tack, F.M.G., 2009. Trace metal behaviour in estuarine and riverine floodplain soils and sediments: a review. Sci. Total Environ. 407, 3972–3985. https://doi.org/10.1016/j.scitotenv.2008.07.025.

Flanagan, K., Branchu, P., Boudahmane, L., Caupos, E., Demare, D., Deshayes, S., Dubois, P., Meffray, L., Partibane, C., Saad, M., Gromaire, M., 2019. Science of the Total Environment Retention and transport processes of particulate and dissolved micropollutants in stormwater bio fi lters treating road runoff 656, 1178–1190. https://doi.org/10.1016/j.scitotenv.2018.11.304.

Fonseca, B., Figueiredo, H., Rodrigues, J., Queiroz, A., Tavares, T., 2011. Mobility of Cr, Pb, Cd, Cu and Zn in a loamy sand soil: a comparative study. Geoderma 164, 232–237. https://doi.org/10.1016/j.geoderma.2011.06.016.

Haq, S., Kaushal, S.S., Duan, S., 2018. Episodic salinization and freshwater salinization syndrome mobilize base cations, carbon, and nutrients to streams across urban regions. Biogeochemistry 141, 463–486. https://doi.org/10.1007/s10533-018-0514-2.

Islam, M.A., Angove, M.J., Morton, D.W., Pramanik, B.K., Awual, M.R., 2020. A mechanistic approach of chromium (VI) adsorption onto manganese oxides and boehmite. J. Environ. Chem. Eng. 8, 103515 https://doi.org/10.1016/J.JECE.2019.103515.

Ivanovsky, A., Belles, A., Criquet, J., Dumoulin, D., Noble, P., Alary, C., Billon, G., 2018. Assessment of the treatment efficiency of an urban stormwater pond and its impact on the natural downstream watercourse. J. Environ. Manag. 226, 120–130. https://doi.org/10.1016/j.jenvman.2018.08.015.

Kelly, T.J., Hamilton, E., Watts, M.J., Ponting, J., Sizmur, T., 2020. The effect of flooding and drainage duration on the release of trace elements from floodplain soils. Environ. Toxicol. Chem. 39, 2124–2135. https://doi.org/10.1002/etc.4830.

Kratky, H., Li, Z., Chen, Y., Wang, C., Li, X., Yu, T., 2017. A critical literature review of bioretention research for stormwater management in cold climate and future research recommendations 11, 1–15. https://doi.org/10.1007/s11783–017-0982-y.

Liu, L., Li, W., Song, W., Guo, M., 2018. Remediation techniques for heavy metal-contaminated soils: principles and applicability. Sci. Total Environ. 633, 206–219. https://doi.org/10.1016/j.scitotenv.2018.03.161.

Liu, S., Huang, J.H., Zhang, W., Shi, L.X., Yi, K.X., Zhang, C.Y., Pang, H.L., Li, J.N., Li, S. Z., 2022. Investigation of the adsorption behavior of Pb(II) onto natural-aged microplastics as affected by salt ions. J. Hazard. Mater. 431. https://doi.org/10.1016/j.jhazmat.2022.128643.

Luo, Y., Tan, W., Suib, S.L., Qiu, G., Liu, F., 2018. Dissolution and phase transformation processes of hausmannite in acidic aqueous systems under anoxic conditions. Chem. Geol. 487, 54–62. https://doi.org/10.1016/j.chemgeo.2018.04.016.

Maity, S., Biswas, C., Banerjee, S., Guchhait, R., Adhikari, M., Chatterjee, A., Pramanick, K., 2021. Interaction of plastic particles with heavy metals and the resulting toxicological impacts: a review. Environ. Sci. Pollut. Res. 28, 60291–60307. https://doi.org/10.1007/s11356-021-16448-z/Published.

McKenzie, E.R., Nyquist, J., Ryan, R., Toran, L., Beganskas, S., Caplan, J., Eisenman, S., Behbahani, A., Donaghue, A., Pope, G., 2019. I-95 Girard Avenue Interchange Stormwater Project Annual Report: Sept 2018 to Sept 2019.

McManus, M., Davis, A.P., 2020. Impact of periodic high concentrations of salt on bioretention water quality performance. J. Sustain. Water Built Environ. 6, 1–11. https://doi.org/10.1061/JSWBAY.0000922.

Miranda, L.S., Ayoko, G.A., Egodawatta, P., Goonetilleke, A., 2022. Adsorption-desorption behavior of heavy metals in aquatic environments: influence of sediment, water and metal ionic properties. J. Hazard. Mater. 421. https://doi.org/10.1016/j.jhazmat.2021.126743.

Mullins, A.R., Bain, D.J., Pfeil-McCullough, E., Hopkins, K.G., Lavin, S., Copeland, E., 2020. Seasonal drivers of chemical and hydrological patterns in roadside infiltration-based green infrastructure. Sci. Total Environ. 714, 136503 https://doi.org/10.1016/j.scitotenv.2020.136503.

Nelson, S.S., Yonge, D.R., Barber, M.E., 2009. Effects of road salts on heavy metal mobility in two eastern Washington soils. J. Environ. Eng. 135, 505–510. https://doi.org/10.1061/(asce)0733-9372(2009)135:7(505).

Nieber, J.L., Arika, C.N., Lahti, L., Gulliver, J.S., Weiss, P.T., 2014. The Impact of Stormwater Infiltration Practices on Groundwater Quality 123.

Norrström, A.C., 2005. Metal mobility by de-icing salt from an infiltration trench for highway runoff. Appl. Geochem. 20 (10), 1907–1919. https://doi.org/10.1016/j.apgeochem.2005.06.002.

Obropta, C.C., Kardos, J.S., 2007. Review of urban stormwater quality models: deterministic, stochastic, and hybrid approaches. J. Am. Water Resour. Assoc. 43, 1508–1523. https://doi.org/10.1111/j.1752-1688.2007.00124.x.

Oldham, V.E., Siebecker, M.G., Jones, M.R., Mucci, A., Tebo, B.M., Luther, G.W., 2019. The speciation and mobility of Mn and Fe in estuarine sediments. Aquat. Geochem. 25, 3–26. https://doi.org/10.1007/s10498-019-09351-0.

Oster, J.D., Sposito, G., Smith, C.J., 2016. Accounting for potassium and magnesium in irrigation water quality assessment. Calif. Agric. 70, 71–76. https://doi.org/10.3733/ca.v070n02p71.

Parvej, S., Naik, D.L., Sajid, H.U., Kiran, R., Huang, Y., Thanki, N., 2021. Fugitive dust suppression in unpaved roads: State of the art research review. Sustain 13, 1–22. https://doi.org/10.3390/su13042399.

Paus, K.H., Morgan, J., Gulliver, J.S., Leiknes, T., Hozalski, R.M., 2014. Effects of temperature and NaCl on toxic metal retention in bioretention media. J. Environ. Eng. 140, 04014034 https://doi.org/10.1061/(asce)ee.1943-7870.0000847.

Donald S. Ross, Quirine Ketterings. 2011. Recommended Soil Testing Procedures for Northeastern United States. Cooperative Bulletin, Chapter 9 493: 75–86. ⟨https://s3.amazonaws.com/udextension/lawngarden/files/2012/10/CHAP9.pdf⟩.

Sangiumsak, N., Punrattanasin, P., 2014. Adsorption behavior of heavy metals on biomaterials. Pol. J. Environ. Stud. 23, 853–865. https://doi.org/10.1021/jf0496402.

Søberg, L.C., Viklander, M., Blecken, G.T., 2017. Do salt and low temperature impair metal treatment in stormwater bioretention cells with or without a submerged zone?

Sci. Total Environ. 579, 1588–1599. https://doi.org/10.1016/j.scitotenv.2016.11.179.
Stormwater BMP Database, 2021. URL ⟨https://bmpdatabase.org/bmp-statistical-analysis-tool⟩.
Tang, J., Wang, W., Feng, J., Yang, L., Ruan, T., Xu, Y., 2021. Urban green infrastructure features influence the type and chemical composition of soil dissolved organic matter. Sci. Total Environ. 764, 144240 https://doi.org/10.1016/j.scitotenv.2020.144240.
Tedoldi, D., Chebbo, G., Pierlot, D., Branchu, P., Kovacs, Y., Gromaire, M.C., 2017. Spatial distribution of heavy metals in the surface soil of source-control stormwater infiltration devices – inter-site comparison. Sci. Total Environ. 579, 881–892. https://doi.org/10.1016/j.scitotenv.2016.10.226.
Tomczak, W., Boyer, P., Krimissa, M., Radakovitch, O., 2019. Kd distributions in freshwater systems as a function of material type, mass-volume ratio, dissolved organic carbon and pH. Appl. Geochem. 105, 68–77. https://doi.org/10.1016/j.apgeochem.2019.04.003.
Tessier, A., Campbell, P.G.C., Bisson, M., 1979. Sequential Extraction Procedure for the Speciation of Particulate Trace Metals. Anal. Chem. 51 (7), 844–851. https://doi.org/10.1021/ac50043a017.
US-EPA, 2017a. https://www.epa.gov/dwstandardsregulations.
US-EPA, 2017b. https://www.epa.gov/wqc/national-recommended-water-quality-criteria-aquatic-life-criteria-table.
US-EPA, 2002. Supplemental Guidance for developing soil screening levels for Superfund sites. Office of Solid Waste and Emergency Response (OSWER).
US-EPA, 2003. Guidance for Developing Ecological Soil Screening Levels. URL ⟨https://www.epa.gov/chemical-research/guidance-developing-ecological-soil-screening-levels⟩.
Walaszek, M., Bois, P., Laurent, J., Lenormand, E., Wanko, A., 2018. Micropollutants removal and storage efficiencies in urban stormwater constructed wetland. Sci. Total Environ. 645, 854–864. https://doi.org/10.1016/j.scitotenv.2018.07.156.
Wang, J., Zhang, P., Yang, L., Huang, T., 2016. Cadmium removal from urban stormwater runoff via bioretention technology and effluent risk assessment for discharge to surface water. J. Contam. Hydrol. 185–186, 42–50. https://doi.org/10.1016/j.jconhyd.2016.01.002.
Wei, T., Wijesiri, B., Jia, Z., Li, Y., Goonetilleke, A., 2019. Re-thinking classical mechanistic model for pollutant build-up on urban impervious surfaces. Sci. Total Environ. 651, 114–121. https://doi.org/10.1016/j.scitotenv.2018.09.013.
van Genuchten, M.T., Simunek, J., Toride, N., Sejna, M., 2012. STANMOD: Model Use, Calibration, and Validation. https://doi.org/10.13031/2013.42247.
Wen, X., Lu, J., Wu, J., Lin, Y., Luo, Y., 2019. Influence of coastal groundwater salinization on the distribution and risks of heavy metals. Sci. Total Environ. 652, 267–277. https://doi.org/10.1016/j.scitotenv.2018.10.250.
Wong, V.N.L., Greene, R.S.B., Dalal, R.C., Murphy, B.W., 2010. Soil carbon dynamics in saline and sodic soils: a review. Soil Use Manag. https://doi.org/10.1111/j.1475-2743.2009.00251.x.
Wong, V.N.L., Johnston, S.G., Burton, E.D., Bush, R.T., Sullivan, L.A., Slavich, P.G., 2013. Seawater-induced mobilization of trace metals from mackinawite-rich estuarine sediments. Water Res. 47, 821–832. https://doi.org/10.1016/j.watres.2012.11.009.
Wuana, R.A., Okieimen, F.E., 2011. Heavy metals in contaminated soils: a review of sources, chemistry, risks and best available strategies for remediation. ISRN Ecol. 2011, 1–20. https://doi.org/10.5402/2011/402647.
Zhang, W., Tsang, D.C.W., 2013. Conceptual framework and mathematical model for the transport of metal-chelant complexes during in situ soil remediation. Chemosphere 91, 1281–1288. https://doi.org/10.1016/j.chemosphere.2013.02.034.
Zou, X., Li, Y., Wang, L., Ahmed, M.K., Chen, K., Wu, J., Xu, Y., Lin, Y., Xiao, X., Chen, B., Wu, K., Liu, J., Lin, F., 2022. Distribution and assessment of heavy metals in suspended particles in the Sundarban mangrove river, Bangladesh. Mar. Pollut. Bull. 181. https://doi.org/10.1016/j.marpolbul.2022.113856.